

Article

Optimal Balance between Heating, Cooling and Environmental Impacts: A Method for Appropriate Assessment of Building Envelope's U-Value

Safieddine Ounis ^{1,2}, Niccolò Aste ², Federico M. Butera ², Claudio Del Pero ², Fabrizio Leonforte ²
and Rajendra S. Adhikari ^{2,*}

- ¹ LACOMOFA Laboratory, Department of Architecture, Mohamed Khider University of Biskra, BP 145 RP, Biskra 07000, Algeria; s.ounis@univ-biskra.dz
- ² Architecture, Built Environment and Construction Engineering Department, Politecnico di Milano, Via Ponzio 31, 20133 Milano, Italy; niccolo.aste@polimi.it (N.A.); federico.butera@polimi.it (F.M.B.); claudio.delpero@polimi.it (C.D.P.); fabrizio.leonforte@polimi.it (F.L.)
- * Correspondence: rajendra.adhikari@polimi.it

Abstract: In Europe, the recent application of regulations oriented to zero-energy buildings and climate neutrality in 2050 has led to a reduction in energy consumption for heating and cooling in the construction sector. The thermal insulation of the building envelope plays a key role in this process and the requirements about the maximum allowable thermal transmittance are defined by country-specific guidelines. Typically, high insulation values provide low energy consumption for heating; however, they may also entail a risk of overheating in summer period and thus negatively affect the overall performance of the building. In addition, the embodied energy and related emissions caused by the manufacturing and transportation processes of thermal insulation cannot be further neglected in the evaluation of the best optimal solution. Therefore, this paper aims to evaluate the influence in terms of embodied and operational energy of various walls' thermal insulation thicknesses on residential buildings in Europe. To this end, the EnergyPlus engine was used for the energy simulation within the Ladybug and Honeybee tools, by parametrically conducting multiple iterations; 53 variations of external wall U-value, considering high- and low-thermal-mass scenarios, were simulated for 100 representative cities of the European context, using a typical multifamily building as a reference. The results demonstrate that massive walls generally perform better than lightweight structures and the best solution in terms of energy varies according to each climate. Accordingly, the wall's thermal transmittance for the samples of Oslo, Bordeaux, Rome and Almeria representative of the Continental, oceanic temperate, Mediterranean, and hot, semi-arid climates were, respectively: 0.12, 0.26, 0.42, and 0.64 W/m²K. The optimal solutions are graphically reported on the map of Europe according to specific climatic features, providing a guidance for new constructions and building retrofit.

Keywords: U-value; thermal insulation; energy efficiency; residential building; embodied energy



Citation: Ounis, S.; Aste, N.; Butera, F.M.; Pero, C.D.; Leonforte, F.; Adhikari, R.S. Optimal Balance between Heating, Cooling and Environmental Impacts: A Method for Appropriate Assessment of Building Envelope's U-Value. *Energies* **2022**, *15*, 3570. <https://doi.org/10.3390/en15103570>

Academic Editor: George Kosmadakis

Received: 5 April 2022
Accepted: 11 May 2022
Published: 13 May 2022

Publisher's Note: MDPI stays neutral with regard to jurisdictional claims in published maps and institutional affiliations.



Copyright: © 2022 by the authors. Licensee MDPI, Basel, Switzerland. This article is an open access article distributed under the terms and conditions of the Creative Commons Attribution (CC BY) license (<https://creativecommons.org/licenses/by/4.0/>).

1. Introduction

The building sector accounted for the largest share of both global final energy use (36%) and energy-related CO₂ emissions (37%) in 2020, as compared to other end-use sectors. However, the levels of emissions within the sector are 10% lower than in 2019, reaching lows not seen since 2007 [1]. This decline was driven largely by reduced energy demand due to the COVID-19 pandemic, mainly due to lockdowns, slowing of economies, the difficulties that households and businesses faced in maintaining and affording energy access and the drop in the global industry and construction activities, but also due to the continuous but limited efforts targeting the sector's decarbonization.

Moreover, over the past few years, a steady increase of 3.14% per year in energy demand for cooling in central and southern Europe was recorded; this was due to the effects of climate change, the increase in the required level of comfort and the gradual raising of thermal insulation of building envelopes [2]. In fact, climate change is expected to gradually reduce the heating demand in northern and north-western Europe, while increasing cooling consumption in southern Europe, accentuating peaks in power demand in summer [3]. At the same time, the electrical load in winter is expected to rise due to the gradual replacement of gas boilers by heat pumps [4].

In addition, the production, transportation and use of all construction materials for buildings resulted in energy and process CO₂ emissions of 3.5 Gt in 2019, or 10% of all energy sector emissions, leading to the abovementioned 38% of global emissions [5].

In such a framework, in order to meet current EU goals, i.e., to reduce the primary energy consumption by 80% and achieve climate neutrality by 2050 [6,7], it is necessary to transform constructions from inefficient energy consumers into net-zero carbon buildings. This new paradigm must be applied not only to new buildings but also to existing ones, which must be subjected to deep renovation with a yearly rate equal at least to 2.5% instead of the current value of 1% [8]. Thus, it is necessary to foster renovation activities by boosting the market uptake of cost-effective solutions. As is well known, building envelope insulation is one of the main solutions that mostly impact the building's energy consumption. Moreover, in the field of renovation, this is one of the main and most effective intervention measures [9]. However, while adding a thermal insulation to exterior walls can reduce heating requirements by up to 70% [10], in some contexts, it may lead to overheating in cooling periods. Simplistic approaches can lead to over-zealousness, according to which "the more insulation the better", but this is not always the case. It is therefore necessary to define the thickness threshold to ensure a balance between different needs [6–11]. Of course, the effectiveness of the insulation layer is also related to the thermal inertia, since it affects the way in which a building reacts to changes in external and internal conditions, influencing its actual thermal load patterns (sensible load for heating and cooling) [12].

Furthermore, a comprehensive process for determining the best thickness of wall thermal insulation also requires an in-depth look at embodied energy, which can even be a major factor in the overall lifecycle energy balance.

In fact, according to a literature review, even if the operational and embodied energy for the existing building stock account for about 90–70% and 10–30%, respectively [13], the embodied impact (e.g., embodied energy and carbon) could increase considerably, up to 74%, for construction characterized by high energy efficiency [14].

Nevertheless, the evaluation of the optimal insulation thickness is generally defined according to the energy saving in the operational phase [15] or adopting the global cost approach introduced by the European Directive 2010/31/EU [11,16,17]. However, such methods do not consider the entire life cycle of the construction components, from the acquisition of raw materials to dismissal. It would be paradoxical to increase the efficiency of buildings through over-insulation of the envelope without at the same time considering the embodied emission of the adopted material.

The evaluation of the optimal thermal transmittance of the building envelope thus has a pivotal role in the lifecycle primary energy saving. In such a respect, recently, this goal has been addressed in various studies [18–25], by optimizing thermal insulation thickness of walls with regard to its influence on the lifecycle assessment. Among them, some research works addressed the energy calculation through simplified simulation tools adopting a steady-state process [18–20], while few used a more accurate method taking into consideration the building's morphology, transient behaviour and operation settings [21–25].

However, none of them provide an extensive evaluation along Europe based on embodied and operational energy, using a dynamic energy-simulation model.

With the aim of identifying the best optimal exterior-wall insulation thickness and thus to obtain a suggested U-value map for the European context, the present work analyses the

overall influence of this insulation in residential buildings by taking climate diversity in Europe as a field of investigation. The outcomes provide recommendations in accordance with 2012/31/EU legislation and a methodology that can be used to define key parameters related to the optimization of buildings' energy efficiency.

2. Research Methodology

As introduced, the present work evaluates the influence of exterior walls' insulation level on the energy performance of residential buildings with the aim to map out a U-value recommendation in the European context.

In more detail, the thermal energy demand assessment (heating and cooling) was simulated using Rhinoceros' Grasshopper parametric interface via the environmental plugins Ladybug and Honeybee [26]. These tools are based on the EnergyPlus simulation engine [27], a worldwide-validated energy simulation tool renowned for its calculation accuracy. During the implementation of the algorithm in Grasshopper, an approach was developed to simulate the total number of iterations following a brute-force method in order to increase the robustness of the study and reduce uncertainties.

The simulation has been carried out in 2 different steps:

- Step 1: 53 options in terms of insulation thickness (ranging from 2 to 20 cm, with a decrement of $0.01 \text{ W/m}^2\text{K}$ between each option) have been performed adopting two possible construction solutions, with low and high thermal mass, respectively, in order to identify the impact of thermal inertia; the evaluation was carried out for 4 selected locations, representative of Continental, oceanic temperate, Mediterranean, and hot, semi-arid climate, respectively.
- Step 2: in the second step, since the residential building stock in Europe is predominantly characterized by masonry walls with medium-high thermal mass [28], a total of 5300 simulations, i.e., 53 predefined insulation thicknesses for 100 representative locations in the whole Europe, have been performed only considering the heavyweight solution. Then, the optimal U-values for external walls, as verified by analysis, were reported on a map of Europe to provide guidance about optimal solutions according to different contexts.

As already introduced, the performance of the insulation has been evaluated considering both the embodied energy (from cradle to gate) related to different thickness as well as the energy due to operation over a calculation period of 30 years. The latter can be considered equal to the lifespan of the insulation material, as suggested by 2012/C115/01 guidelines. In detail, the operational primary energy has been calculated assuming an HVAC system based on an electric vapour-compression ground source heat pump (GSHP) for climates with a number of heating degrees-days (HDD) lower than 2000 and an air source heat pump (ASHP) for climates characterized by HDD equal or greater than 2000. This threshold was selected analysing several studies in the literature reporting a comparison of the cost effectiveness of ASHPs and GSHPs, according to which the payback time of the latter becomes too long, typically above 2000 HDD [28].

It must be noted that the choice to adopt vapour-compression heat pumps as thermal generators is due to the fact that such a technology is one of the most interesting options to replace conventional systems based on fossil fuels in order to reduce the energy demand of buildings.

More in detail, the COP (coefficient of performance) and the EER (energy-efficiency ratio) of the assumed heat pumps were determined considering average values from literature, as shown in the Figure 1. In addition, water distribution and emission subsystems were assumed in the building, considering generation temperatures for hot and chiller water equal to $40 \text{ }^\circ\text{C}$ and $7 \text{ }^\circ\text{C}$ in heating and cooling, respectively. Such temperatures are compatible with radiant heating systems and with air cooling systems (e.g., fan coils), which are versatile solutions that can meet the heating and cooling load in every analysed climatic condition. According to these assumptions, the overall distribution, emission and control efficiency was set to 0.91. As a consequence, the yearly electricity consumption

of the system was calculated and finally the primary energy was determined considering the average electricity to primary energy conversion factor for OECD countries, equal to 2.5 kWh_{ep}/kWh_{el} [29]. Therefore, on the basis of these assumptions, the final energy consumption relevant to the operational phase is calculated using Equation (1):

$$\begin{aligned}
 & \text{Primary energy consumption} \\
 &= \left(\frac{\text{Heating energy demand}}{\text{COP}} + \frac{\text{Cooling energy demand}}{\text{EER}} \right) \\
 &\times \text{Overall efficiency (Distribution, emission and control)} \times \text{Primary energy factor}
 \end{aligned} \tag{1}$$

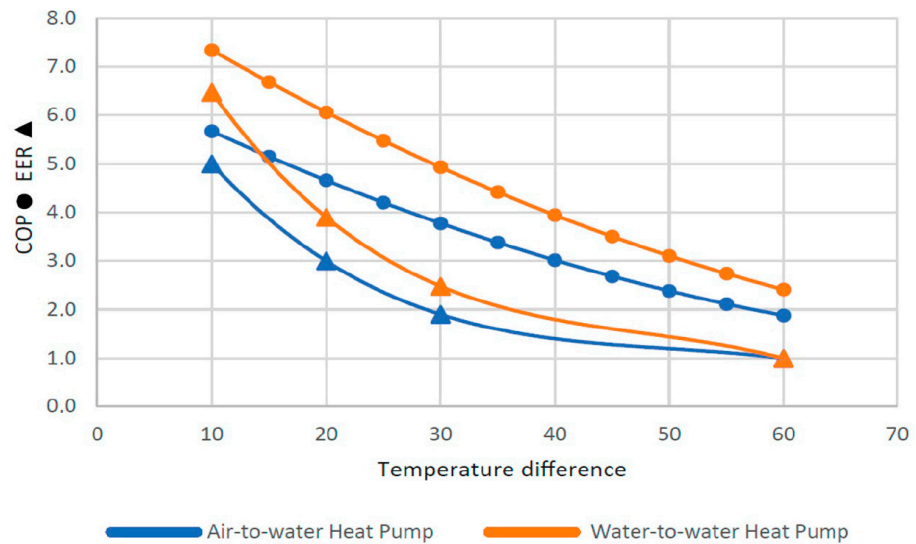


Figure 1. COP and EER reference trends as a function of temperature difference between sources.

The above-described research methodology is summarized in the diagram presented in Figure 2.

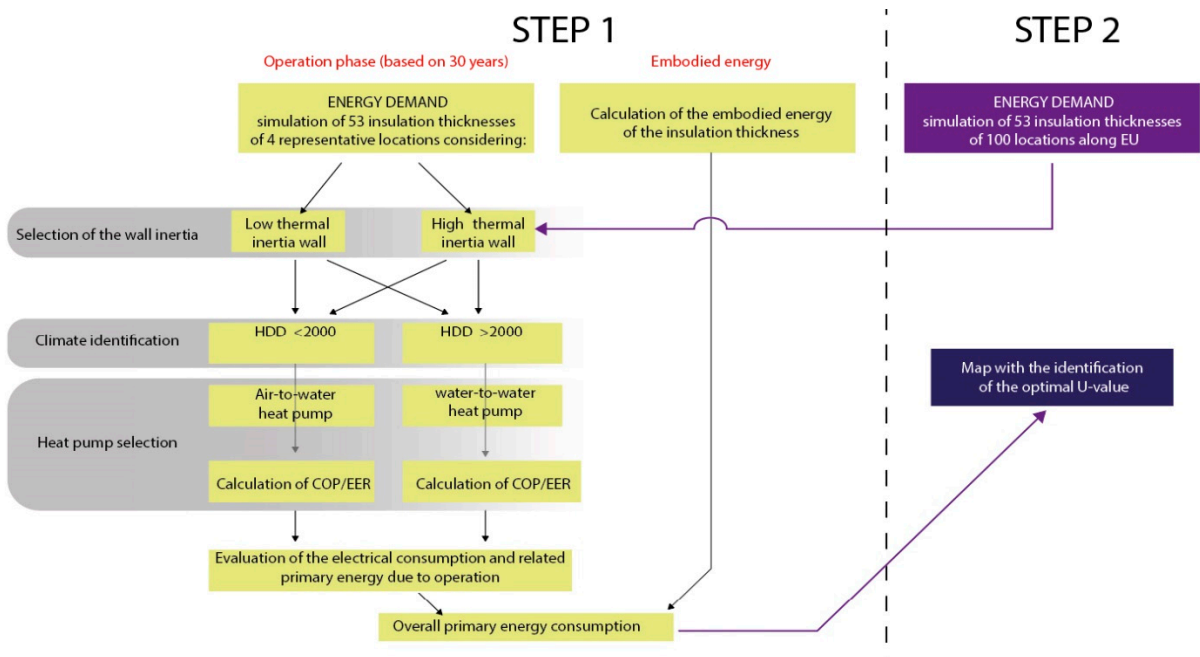


Figure 2. Research methodology workflow.

2.1. Contextual Definition

In order to carry out a general “optimal U-value mapping” referring to the European area, a selection process has been developed with the aim of defining the locations to be studied, which can be considered as representative of the entire European context.

To this aim, the selection process of the representative locations, identified with specific cities, was based on the Köppen–Geiger climate classification as well as on the HDD and cooling degree-day (CDD) values. First, the climate classification for each country was performed. According to the obtained results, at least one location of each climate per country was selected from the list provided by the World Meteorological Organization [30]. If more than one city was listed in the abovementioned weather database, the two characterized by minimum and maximum HDD were selected, while for countries with a wide range of climatic conditions, additional cities with an intermediate climate between the 2 extremes were also included to better represent the country’s context. If some contexts were not represented from [30], the meteorological data were retrieved from the Meteororm database [31]. According to such a methodology, at the end of the process, out of 282 cities of 50 countries, a set of 100 cities able to reproduce the large variety of environmental conditions at the continental scale was selected as shown in Figure 3.

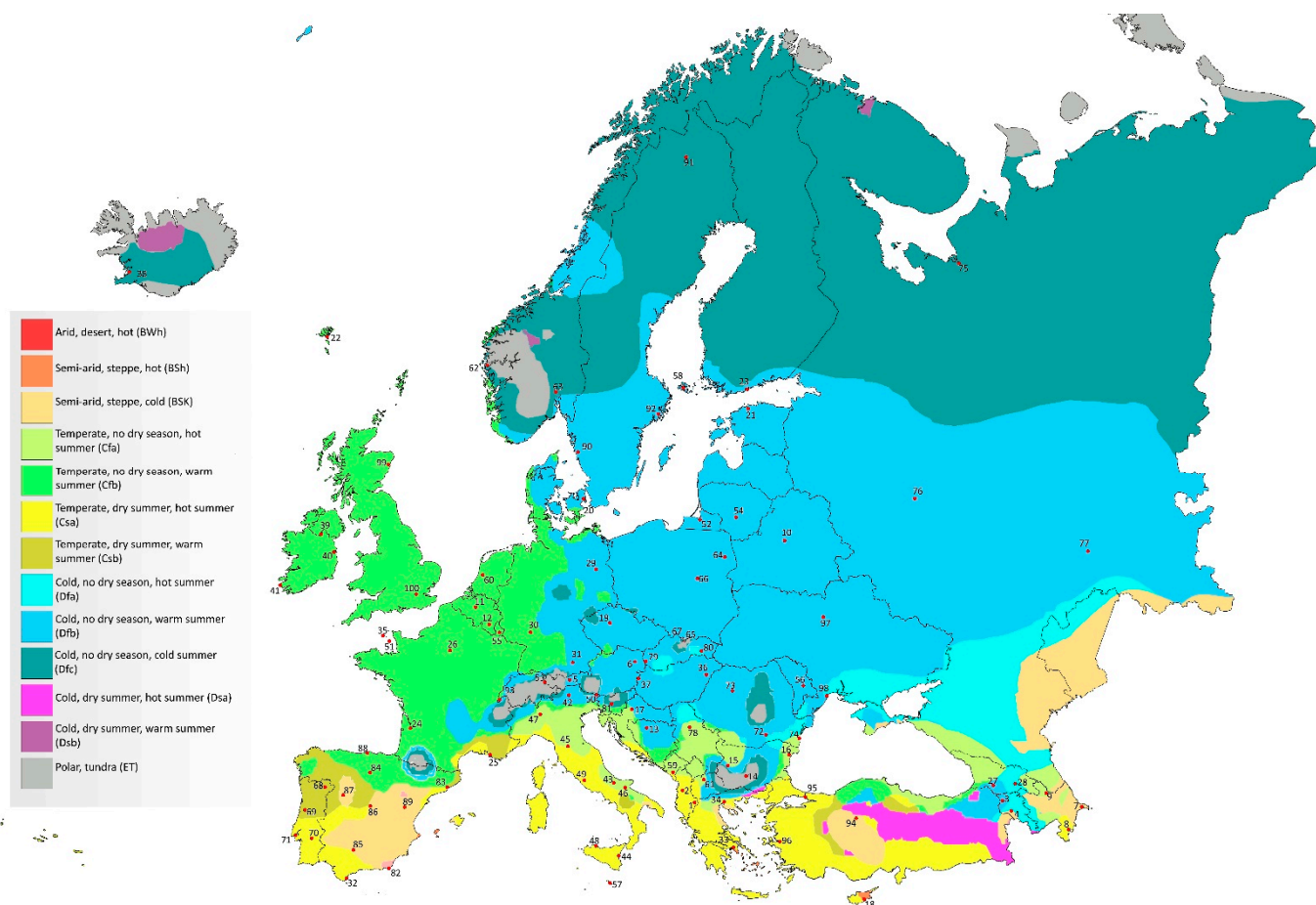


Figure 3. Position of the 100 representative locations. Different colours indicate different Köppen–Geiger classes [32].

In Table 1, the 100 representative locations are listed, followed by the related sub-climate type, their respective HDD and CDD values (calculated with reference to 20 °C and 24 °C respectively), as well as the yearly average temperature extracted from each corresponding weather data file.

Table 1. Heating and cooling degree-days, yearly average temperature and identification for the 100 selected locations in Europe sorted by country and climate type (darker colours means higher HDD/CDD values).

Country	Location	ID	Sub-Climate	HDD20	CDD24	Yearly Average T (°C)	Country	Location	ID	Sub-Climate	HDD20	CDD24	Yearly Average T (°C)
Albania	Korca	1	Csb	3140	108	12.1	Jersey	Jersey	51	Cfb	3231	3	11.2
	Tirana	2	Csa	2030	253	15.8	Latvia	Riga	52	Dfb	4581	10	7.7
Armenia	Gyumri	3	Dfb	5195	39	6.2	Liechtenstein	Vaduz	53	Cfb	3391	54	11.0
	Yerevan	4	Dfa	3251	402	13.0	Lithuania	Kaunas	54	Dfb	4906	14	6.9
Austria	Innsbruck	5	Dfc	4012	38	9.0	Luxemburg	Luxemburg	55	Cfb	3684	31	10.2
	Vienna	6	Cfb	3864	52	10.0	Moldova	Chisinau	56	Dfb	3504	149	11.5
Azerbaijan	Baku	7	Bsk	2409	321	15.2	Malta	Valetta	57	Csa	1101	283	19.0
	Lankaran	8	Csa	2343	253	15.4	Man Island	Castletown	58	Cfb	3463	0	10.6
	Sheki	9	Dfb	2913	7975	13.0	Montenegro	Podgorica	59	Cfa	2318	240	15.1
Belarus	Minsk	10	Dfb	5120	10	6.3	The Netherlands	Amsterdam	60	Cfb	3751	15	10.0
Belgium	Brussels	11	Cfb	3632	24	10.3	North Macedonia	Skopje	61	Cfb	3142	263	12.7
	Saint Hubert	12	Cfb	4547	1	7.5	Norway	Bergen	62	Cfb	4756	4	7.1
Bosnia and Herzegovina	Banja Luka	13	Cfb	3549	92	10.8		Oslo	63	Dfb	4973	4	6.7
Bulgaria	Plovdiv	14	Cfa	3059	175	2.7	Poland	Bialystok	64	Dfb	4931	16	6.9
	Sofia	15	Cfb	3742	64	10.2		Kasprowy W. Mt.	65	ET	7550	0	-0.7
	Varna	16	Cfa	3121	74	12.1		Warsaw	66	Cfb	4367	26	8.4
Croatia	Zagreb	17	Cfb	3293	140	11.8		Zakopane	67	Dfb	5381	3	5.5
Cyprus	Larnaca	18	Csa	1183	379	19.4	Portugal	Braganca	68	Csb	3028	112	12.4
Czech Republic	Prague	19	Cfb	4462	24	8.1		Coimbra	69	Csb	1855	123	15.3
Denmark	Copenhagen	20	Cfb	4348	3	8.3		Evora	70	Csa	1926	208	15.8
Estonia	Tallinn	21	Dfb	4960	79	6.7		Lisboa	71	Csa	1601	174	16.3
Faroe Islands	Torshavn	22	Csc	4713	0	7.1	Romania	Bucharest	72	Cfa	3713	148	10.8
Finland	Helsinki	23	Dfb	5545	8	5.2		Cluj-Napoca	73	Cfb	4288	38	8.5
France	Bordeaux	24	Cfb	2683	78	13.2		Constanta	74	Cfa	3201	62	12.0
	Marseille	25	Csa	2274	153	14.8	Russia	Arkhangelsk	75	Dfb	6841	8	1.6
	Paris	26	Cfb	3357	29	11.1		Moscow	76	Dfb	5436	19	5.5
Georgia	Akhaltikhé	27	Dfb	6272	3	2.8		Samara	77	Dfb	5806	39	4.7
	Tbilisi	28	Cfa	2607	252	14.1	Serbia	Belgrade	78	Cfa	3445	125	11.5
Germany	Berlin	29	Cfb	3852	39	9.8	Slovak Republic	Bratislava	79	Cfb	3733	70	10.4
	Mannheim	30	Cfb	3459	73	11.1		Kosice	80	Dfb	4157	46	9.1
	Munich	31	Cfb	4487	31	8.0	Slovenia	Ljubljana	81	Cfb	4046	67	9.2
Gibraltar	Gibraltar	32	Csa	1021	132	18.5	Spain	Almeria	82	BSk	1069	281	18.5
Greece	Athens	33	Csa	1552	350	17.9		Barcelona	83	Csa	1902	86	15.7
	Thessaloniki	34	Cfa	2271	238	15.4		Burgos	84	Csb	3567	52	9.9
Guernsey	Guernsey	35	Cfb	3103	5075	11.5		Cordoba	85	Csa	1531	522	17.5
Hungary	Debrecen	36	Dfb	3819	84	10.2		Madrid	86	Csa	2592	263	14.3
	Szombathely	37	Dfb	3829	63	10.0		Salamanca	87	Csb	3040	120	11.7
Iceland	Reykjavik	38	Cfc	5670	0	4.5		Santander	88	Cfb	1982	16	14.8
Ireland	Clones	39	Cfb	3974	0	9.1		Teruel	89	Cfb	3060	129	11.5
	Dublin	40	Cfb	3725	0	9.8	Sweden	Göteborg	90	Cfb	4988	3	6.5
	Valentia	41	Cfb	3352	0	11.0		Kiruna	91	Dfc	7816	0	-1.1
Italy	Bolzano	42	Dfb	3515	102	10.7		Stockholm	92	Dfb	5037	6	6.5
	Campobasso	43	Cfa	3296	51	11.3	Switzerland	Geneva	93	Cfb	3658	53	10.4
	Catania	44	Csa	1632	211	17.1	Turkey	Ankara	94	Csb	4066	99	9.6
	Florence	45	Csa	2495	172	14.2		Istanbul	95	Csa	2406	120	14.5
	Foggia	46	Cfa	2223	240	15.4		Izmir	96	Csa	1889	350	16.7
	Milan	47	Cfb	3014	113	12.4		Kiev	97	Dfb	4529	34	8.0
	Palermo	48	Csa	1146	203	18.8	Ukraine	Odessa	98	Cfa	3923	69	10.1
	Rome	49	Csa	1994	112	15.8	United Kingdom	Aberdeen	99	Cfb	4267	1	8.4
	Tarvisio	50	Dfb	4681	9	7.0		London	100	Cfb	3683	11	10.2

2.2. Reference Building Model

Multi-storey residential buildings from the second half of the last century—which represent around 20% of the total existing European building stock—offer significant potential for energy renovation [33]. The most common types are 4–5 storey condominium buildings and are generally characterized by very low levels of energy performance (low energy efficiency in heating, ventilation and air-conditioning systems and poor thermal insulation) [34,35]. These building types therefore currently represent an extremely important, if not the most important, mass of intervention. For these reasons, having to take concrete benchmarks, we have referred to them.

In this regard, the energy analysis was performed on a mid-rise residential building of 4 levels with 12 apartments, where only 3 levels are heated/cooled with a conditioned area of 897 m². Such a building has been already studied in different research works, since it is the demonstrator of the recent Horizon 2020 project “HEART” [36], and can be considered representative of multifamily buildings built across Europe between the 1960s and the 1990s [37].

In detail, the building energy model developed in a previous work [36], characterized by an S/V ratio of 0.33 and an overall average WWR of 18% (Figure 4), was used in this research. It is worth mentioning that this model has been calibrated and validated with real measurements, thus guaranteeing the consistency and reliability of the results obtained in terms of energy performance.

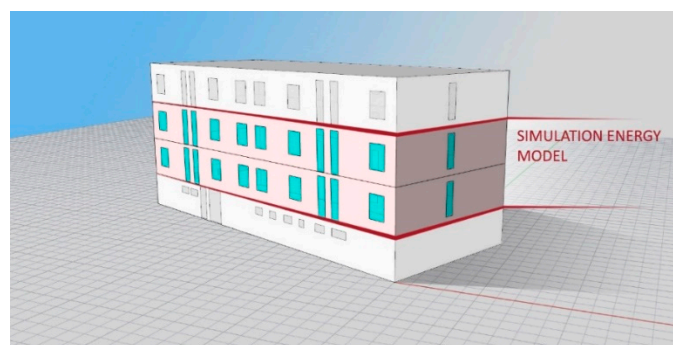


Figure 4. 3D view of the building model on Rhinoceros UI.

In more detail, for the scope of this research, the simulation was carried out solely considering the two juxtaposed intermediate levels, as shown in Figure 4, where each floor was identified with a singular thermal zone while the upper and lower exposed horizontal surfaces are considered as adiabatic. With regard to the windows, in order to focus on the walls' insulation, the features applied in the actual retrofit (within the abovementioned HEART project) were assumed and left unchanged in all the analysed cases.

In this way, it was possible to focus the research only on the aspects of specific interest, without burdening the data with disturbances and interferences that would have weighed down the work without increasing its scientific value.

According to the proposed approach, the overall primary energy consumption was calculated and subsequently reported in Section 3 as the sum of the total values for heating and cooling of the 2 selected floors during the assumed lifetime of 30 years, plus the embodied energy of the material needed to insulate the walls of such portion of the building.

Table 2 shows the boundary conditions of the building energy model, i.e., the thermo-physical properties of the envelope elements, the building use and operating settings to be applied in the energy simulation. Given the residential destination of the building, a variable internal gains (occupancy, equipment and lighting load) profile with a daily average value of 4 W/m^2 as suggested in the Italian building energy design regulation according to the standard variable profile defined by SIA Merkblatt 2024 [38], as shown in Figure 5. In addition, an intermittent ventilation and infiltration profile was set with a value of 0.5 air changes per hour (ACH) during the day and 0.2 ACH during the night, equivalent to diurnal and nocturnal geometric values assessed in the residential building stock in the literature [39]. Such considerations allow a more realistic approach to the changes in interior temperature caused by the fluctuation in the occupancy profiles. Moreover, the heating and cooling set-points were considered, respectively, to be equal to $20 \text{ }^\circ\text{C}$ and $26 \text{ }^\circ\text{C}$ based on the values suggested in EN 15251 [40].

Table 2. Building energy model's thermo-physical and operational parameters.

Simulation Parameters				
Category	Group	Type	Unit	Parameter Input Value
Thermo-physical parameters	Envelope	U-value exterior walls	$\text{W/m}^2\text{K}$	0.12–0.64
		Windows: U-value	$\text{W/m}^2\text{K}$	1.40
		SHGC	-	0.75
Building operation	Activities	Internal load per area (<i>a</i>) daily average. Daily profile in Figure 5	W/m^2	4
	Control and operation settings	Heating set-point temperature	$^\circ\text{C}$	20
		Cooling set-point temperature	$^\circ\text{C}$	26
		Air-change rate ACR (infiltration and natural ventilation)	vol/h	0.5 from 8:01 to 20:00, 0.2 from 20:01 to 8:00

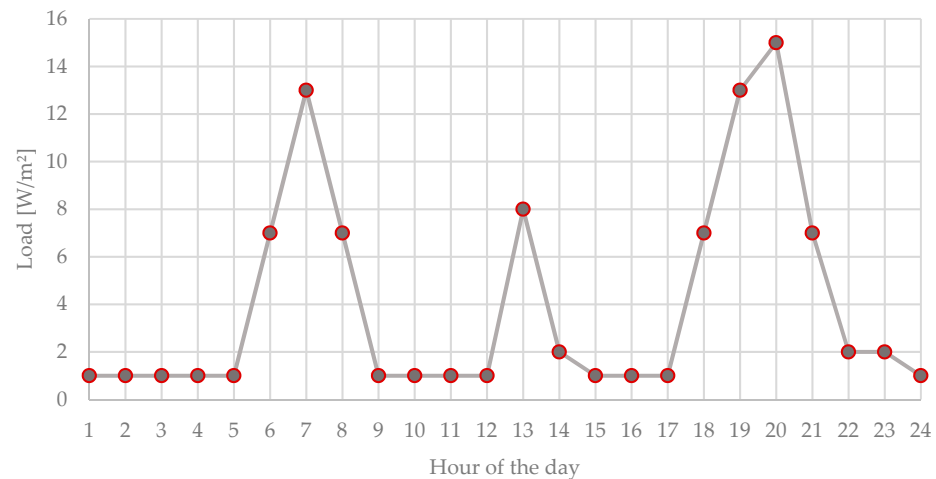


Figure 5. Internal gains daily profile.

In order to showcase the influence of the wall's U-value and dynamic properties on the building energy performance, as a first step, two external uninsulated wall configurations were assumed, with the same U-value of $1.25 \text{ W/m}^2\text{K}$ and different thermal inertia parameters. In detail, a lightweight wall (S1) and a massive wall (S2) with respective decrement factor and time-shift values of $f_1 = 0.98$, $\Delta t_1 = 1.23 \text{ h}$ and $f_2 = 0.12$, $\Delta t_2 = 13.71 \text{ h}$ were considered. The different wall stratifications are shown in Figure 6.

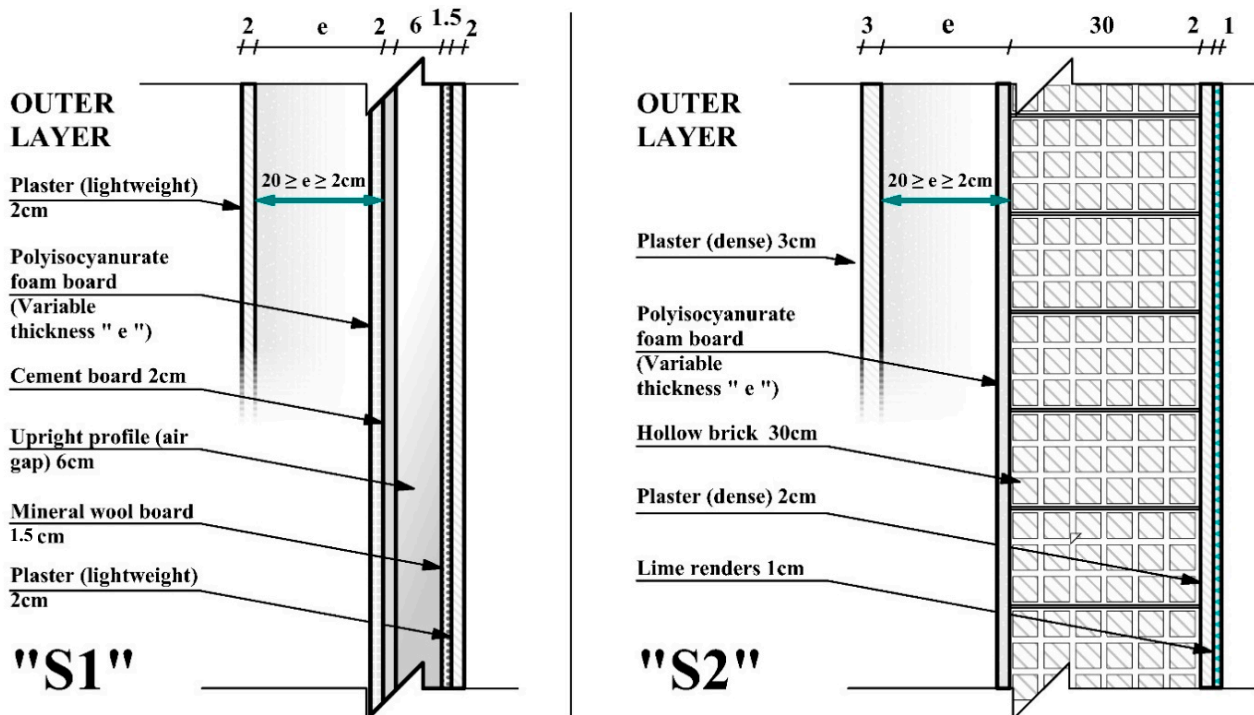


Figure 6. Building's external wall stratifications: scenario "S1": low mass wall; scenario "S2": high mass wall. The outer insulation layer is presented with a variable thickness "e".

Furthermore, the calculation of the insulated wall's U-value, which represents the variable in the building's energy evaluation in this study, was based on an incremental criterion according to the insulation thickness. In more detail, the application of polyisocyanurate foam sheets as continuous insulation was assumed with a variable thickness from 2 to 20 cm, as shown in Figure 7. In addition to its widespread use in the European market [41], this insulation material presents a high thermal resistance with good long-term durability ($\rho = 35 \text{ kg/m}^3$, $c = 1.4 \text{ kJ/kgK}$, $\lambda = 0.026 \text{ W/mK}$) [15]; furthermore, its simple installation

process allows for applications on both new constructions and refurbishment works, while from an embodied energy point of view, it is characterized by an energy impact equal to 19.16 kWh/kg (from cradle to gate) [15].

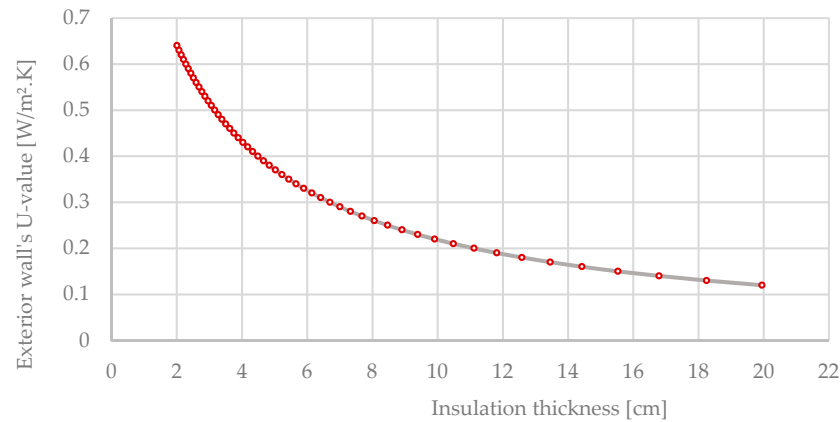


Figure 7. External-wall insulation thickness and related U-value.

According to the above-described approach, and considering the limits set by the insulation's commercial thicknesses (from 2 cm to 20 cm), a U-value range, with a lower bound of 0.12 W/m²K for a highly insulated wall and an upper bound of 0.64 W/m²K for a poorly insulated wall was obtained through the Equation (2):

$$U_{\text{ext}} = \frac{1}{R_{sx} + R_{ins} + R_{se} + R_{si}} \quad (2)$$

where:

U_{ext} : is the thermal transmittance of the external wall (W/m²K);

R_{si} and R_{se} : are the interior and exterior wall superficial resistances (m²K/W);

R_{sx} : is the thermal resistance (m²K/W) of the non-insulated walls (S1, S2) presented in Figure 6;

R_{ins} : is the insulation layer's thermal resistance (m²K/W) equals to: $R_{ins} = e/\lambda$.

Based on this equation, different wall U-values were calculated while maintaining an increment of 0.01 W/m²K, as shown in Figure 7, by adopting the consequent Equation (3):

$$e = \lambda \times \left[\frac{1}{U_{\text{ext}}} - (R_{sx} + R_{se} + R_{si}) \right] \quad (3)$$

3. Energy Analysis

This section describes the results of the energy analysis, carried out firstly on four representative climatic conditions and then on the entire European context.

3.1. Step 1: Simulation in Respect of 4 Representative Climate

In this section, the analysis on the influence of each external walls' configuration on the building's energy performance was performed, by comparing the two selected types of walls, namely S1 and S2; the results obtained from this first assessment were used to calculate the primary energy consumption as well as the embodied energy for the 100 addressed locations.

In more detail, with the main aim to investigate the influence of thermal mass on building's energy performance within European climatic contexts, four cities were considered as representative examples of the cold (continental), moderate (oceanic temperate), warm (Mediterranean) and hot regions (hot semiarid), namely: Oslo (Norway), Bordeaux (France), Rome (Italy), Almeria (Spain). The achieved results, shown in Figure 8, are presented in terms of lifecycle energy, i.e., heating and cooling primary energy consumption on a 30-year lifespan plus embodied energy, as a function of the external wall's U-value.

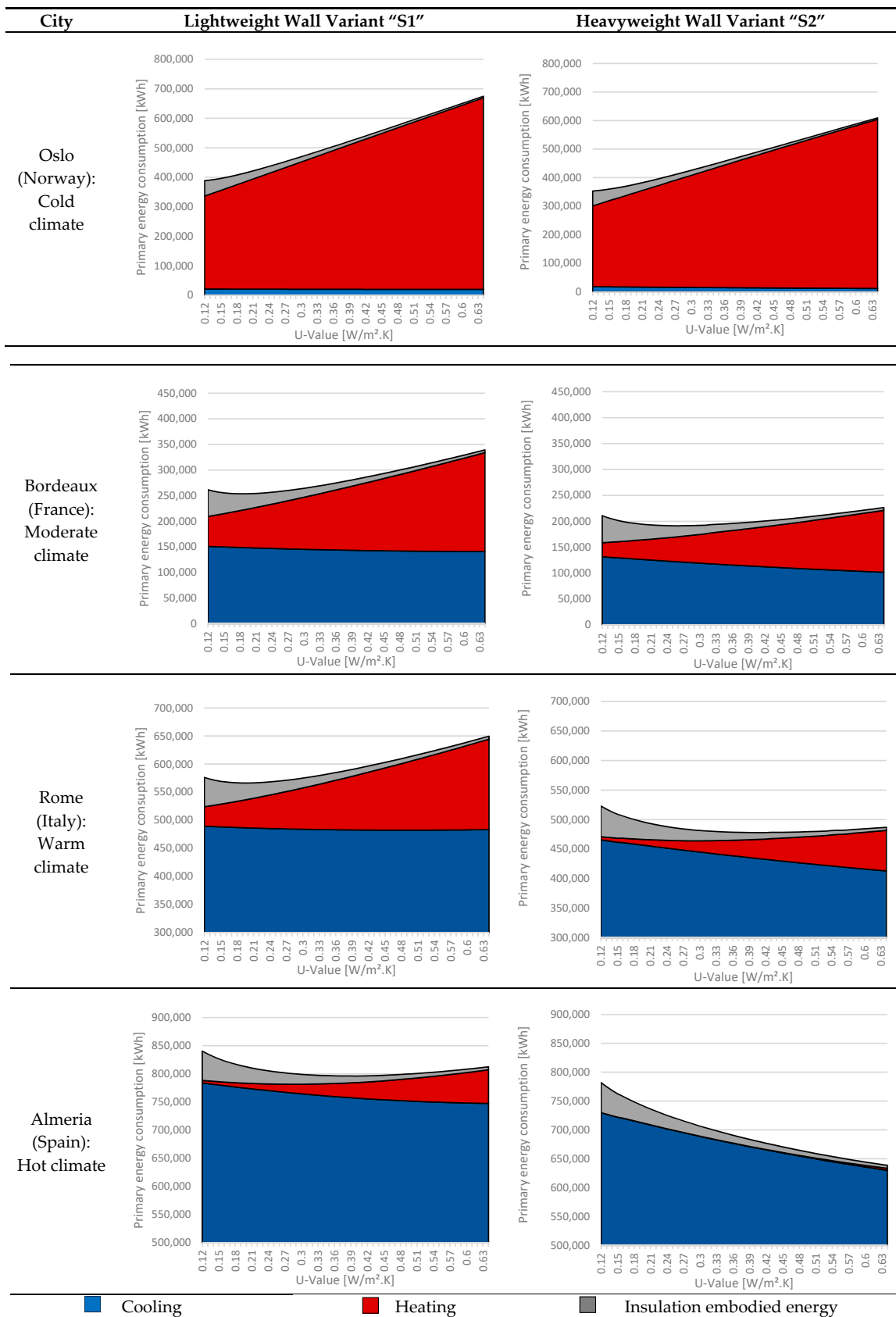


Figure 8. Building primary energy consumption in terms of heating and cooling for the four representative cities of the European context (Oslo, Bordeaux, Rome and Almeria).

- Results for Oslo

As reported in the charts, for both cases of lightweight S1 and heavyweight S2 solutions, the results show a great decrease in total energy consumption of about 50% from the upper to lower bounds of U-value. Moreover, the consumption due to operation only is reduced from 670 to 330 MWh, and from 605 to 300 MWh, respectively, considering the lightweight and heavyweight walls. Thus, it should be noted that the massive solution allows an energy saving of about 10% in comparison to the lightweight one. Due to the cold winter and mild summer that characterize this climate, the thermal energy consumption is mostly dedicated to heating (93% to 97% of the total operational consumption) that diminishes while decreasing the wall's U-value, with an almost negligible cooling requirement in all conditions. Of course, since the climate is characterized by high HDD, considering 30 years of consumption due to operation, the share of the embodied energy of the material on the overall energy need is quite small; it varies from 5.2 MWh and 52 MWh from 2 cm to 20 cm of insulation, with a relative impact on the overall energy consumption between 1% and 13%, respectively, regardless of the walls' inertia. In such a specific climate, the best optimal insulation thickness in terms of overall consumption is equal to 20 cm, which allows to achieve a U-value equal to $0.12 \text{ W/m}^2\text{K}$.

- Results for Bordeaux

Similarly, for Bordeaux, the results show that the energy consumption for operation decreases with a higher level of insulation for both wall constructions S1 and S2, with minimum values equal to 210 and 160 MWh, respectively, with a saving of 24% considering the massive wall instead of lightweight wall. Moreover, by lowering the U-value, we distinguish that for S1, the decrease in heating energy consumption is relatively higher than the increase in cooling; however, for S2, both trends are similar, with a more defined increase in cooling in comparison to that of the lightweight solution. In such a context, the impact due to embodied energy increases in comparison to the abovementioned climate and varies from 1 to 20% of the total in lightweight wall and from 2 to 25% for a heavyweight wall. Instead of a linear trend, therefore, we see an inflection, with an intermediate minimum point. The insulation thickness able to minimize the overall consumption is thus equal to 12 cm ($0.18 \text{ W/m}^2\text{K}$) and 8 cm ($0.26 \text{ W/m}^2\text{K}$) considering variant S1 and S2, respectively.

- Results for Rome

For Rome, just considering the operational energy, the maximum insulation thickness of 20 cm is also the best solution for lightweight option S1, where the energy consumption achieves the lowest value of 525 MWh. In this condition, the cooling attains a predominant impact of 93% of the building's energy consumption, slightly diminishing with the growth of the wall's U-value. Such a trend in cooling performance, however, is not balanced by the heating trend, which increases from 35 MWh to 160 MWh, respectively, moving from the lowest to highest U-value. Considering the overall energy consumption, the optimal U-value is equal to $0.2 \text{ W/m}^2\text{K}$, achievable with 11 cm of insulation.

The results for S2 are characterized by an initial lower yearly energy consumption with minimized cooling and heating compared to S1 due to the wall's thermal inertia contribution. However, as it draws an inflection as a function of the incremental evolution of the wall's U-value, a slight reduction in the energy consumption from 470 MWh with 20 cm of insulation to about 460 MWh with a thickness of 8 cm can be noticed. It should also be noted that in such a temperate climate, the over-insulation of massive walls allows a slightly decrease in the heating consumption but a non-negligible increase in the cooling one.

However, even if the abovementioned reduction of operative energy can be considered almost negligible (2%), an energy saving in terms of embodied energy can be achieved. The trend inflection is even more striking considering the overall primary energy consumption, which also takes into account the impact of the energy embodied in the insulation material. In such a respect, the optimal insulation thickness that allows to minimize the overall primary energy consumption is equal to 4 cm (U-value equal to $0.42 \text{ W/m}^2\text{K}$).

- Results for Almeria

For the lightweight variant S1, the building's yearly energy consumption initially decreases exponentially in proportion to the incremental reduction in the external wall's U-value from 810 MWh (at 0.64 W/m²K), until it reaches an operative energy optimum of 780 MWh/m²y at 0.25 W/m²K (5% of energy saving). After that, the energy consumption grows gradually by lowering the U-value; in detail, although the heating energy consumption diminishes from 12 to 4 MWh, the cooling energy consumption accounts for 91 to 99% of the operative energy consumption and increases considerably on the lowest U-value. Such a phenomenon is related, first, to the hot summers characterizing the climate, and second, to the wall's over-insulation effect, as the heat gains induced by solar and internal gains tend to remain inside the building envelope.

However, the insulation thickness that allows to optimize the overall energy consumption for cooling, heating and embodied energy is equal to 4 cm, which corresponds to a U-value of about 0.5 W/m²K. In such a condition the impact of the embodied energy is about 1% of the total, while the share due to heating and cooling is about 4% and 96%, respectively.

Different results were achieved for the S2 scenario, since heating consumption can be considered negligible. The most efficient solution in terms of overall energy consumption is equal to the highest addressed U-value (equal to 0.64 W/m²K), achievable with the minimum insulation thickness of 2 cm.

According to obtained outcomes, it is possible to conclude that the external wall's energy-efficient U-value is highly influenced by the wall's thermo-dynamic properties. In fact, the lightweight wall system S1 generally requires a relatively lower U-value compared to S2, electing the latter as the most suitable solution in terms of energy saving for the European context overall. In detail, for the four studied cities, lower heating and cooling values were observed due to the thermal mass effect on dampening the fluctuations in temperature, thus avoiding cooling peaks and also minimizing heating requirements with interior heat dissipation during the cold periods. Moreover, it should be noted that the share of impact of embodied energy on the overall primary energy consumption is climate dependent: in heating-dominated regions, generally characterized by high operation energy, the embodied energy represents a smaller percentage in the life-cycle energy use, while in temperate climates, the impact due to the material is pivotal in order to define the best optimal solution.

3.2. Step 2: Simulation on the 100 Representative Cities of Europe

In the second step of the work, the process carried out for the four reference cities was extended to 100 representative cities in Europe. As already mentioned, according to the results obtained in step 1 and considering that the residential building stock in Europe is predominately characterized by masonry walls with medium–high thermal mass [28], the analysis was carried out just on the heavyweight wall option. The obtained results are reported in Table 3.

Table 3. External wall optimal U-value for the 100 selected locations in Europe (darker colours means higher U values).

Country	Location	ID	External Wall's Optimal U-Value [W/m ² K]	Country	Location	ID	External Wall's Optimal U-Value [W/m ² K]
Albania	Korca	1	0.22	Jersey	Jersey	51	0.20
	Tirana	2	0.32	Latvia	Riga	52	0.12
Armenia	Gyumri	3	0.13	Liechtenstein	Vaduz	53	0.17
	Yerevan	4	0.18	Lithuania	Kaunas	54	0.12
Austria	Innsbruck	5	0.16	Luxemburg	Luxemburg	55	0.15
	Vienna	6	0.13	Moldova	Chisinau	56	0.16
Azerbaijan	Baku	7	0.25	Malta	Valetta	57	0.64
	Lankaran	8	0.24	Man Island	Castletown	58	0.18
	Sheki	9	0.20	Montenegro	Podgorica	59	0.28

Table 3. Cont.

Country	Location	ID	External Wall's Optimal U-Value [W/m ² K]	Country	Location	ID	External Wall's Optimal U-Value [W/m ² K]
Belarus	Minsk	10	0.12	The Netherlands	Amsterdam	60	0.15
Belgium	Brussels	11	0.16	North Macedonia	Skopje	61	0.18
	Saint Hubert	12	0.12	Norway	Bergen	62	0.12
Bosnia and Herzegovina	Banja Luka	13	0.16		Oslo	63	0.12
Bulgaria	Plovdiv	14	0.18	Poland	Bialystok	64	0.12
	Sofia	15	0.15		Kasprowy Wierch Mt.	65	0.12
	Varna	16	0.18		Warsaw	66	0.13
Croatia	Zagreb	17	0.18		Zakopane	67	0.12
Cyprus	Larnaca	18	0.64	Portugal	Braganca	68	0.27
Czech Republic	Prague	19	0.12		Coimbra	69	0.63
Denmark	Copenhagen	20	0.12		Evora	70	0.58
Estonia	Tallinn	21	0.12		Lisboa	71	0.64
Faroe Islands	Torshavn	22	0.13	Romania	Bucharest	72	0.15
Finland	Helsinki	23	0.12		Cluj-Napoca	73	0.14
France	Bordeaux	24	0.26		Constanta	74	0.17
	Marseille	25	0.33	Russia	Arkhangelsk	75	0.12
	Paris	26	0.17		Moscow	76	0.12
Georgia	Akhaltsoikhé	27	0.12		Samara	77	0.12
	Tbilisi	28	0.22		Belgrade	78	0.16
Germany	Berlin	29	0.14	Serbia			
	Mannheim	30	0.16	Slovak Republic	Bratislava	79	0.15
	Munich	31	0.13		Kosice	80	0.13
Gibraltar	Gibraltar	32	0.64	Slovenia	Ljubljana	81	0.13
Greece	Athens	33	0.49	Spain	Almeria	82	0.64
	Thessaloniki	34	0.30		Barcelona	83	0.39
Guernsey	Guernsey	35	0.23		Burgos	84	0.17
Hungary	Debrecen	36	0.14		Cordoba	85	0.64
	Szombathely	37	0.14		Madrid	86	0.29
Iceland	Reykjavik	38	0.12		Salamanca	87	0.23
Ireland	Clones	39	0.16		Santander	88	0.40
	Dublin	40	0.16	Sweden	Teruel	89	0.21
	Valentia	41	0.19		Gothenburg	90	0.12
Italy	Bolzano	42	0.15		Kiruna	91	0.12
	Campobasso	43	0.18	Switzerland	Stockholm	92	0.12
	Catania	44	0.47		Geneva	93	0.16
	Florence	45	0.22	Turkey	Ankara	94	0.14
	Foggia	46	0.24		Istanbul	95	0.23
	Milan	47	0.16		Izmir	96	0.42
	Palermo	48	0.64	Ukrain	Kiev	97	0.12
	Rome	49	0.42		Odessa	98	0.14
	Tarvisio	50	0.12	United Kingdom	Aberdeen	99	0.14
					London	100	0.16

3.3. Step 3: Elaboration of the Optimal U-Value Map

Taking into consideration the achieved results for the studied cases, an optimal U-value map for the entire European context was elaborated and is presented in Figure 9. In detail, each of the 100 cities is pinpointed on the map and is assigned a colour specific to its respective optimal U-value, in reference to a prior developed colour gradient according to the increment of 0.01 from 0.12 to 0.64 W/m²K. Subsequently, a linear interpolation method was adopted and graphically performed in order to estimate the unknown U-values in between two adjacent points, specific to the two nearest analysed cities.

As can be seen, the values fluctuate between 0.12 and 0.64 W/m²K, decreasing, approximately, with increasing latitude. Basically, this confirms the initial hypothesis suggesting that insulation has a significant positive impact on heat-dominated buildings but must be carefully balanced in warm climates to avoid overheating effects. Finally, the importance of embodied energy cannot be overlooked in all this.

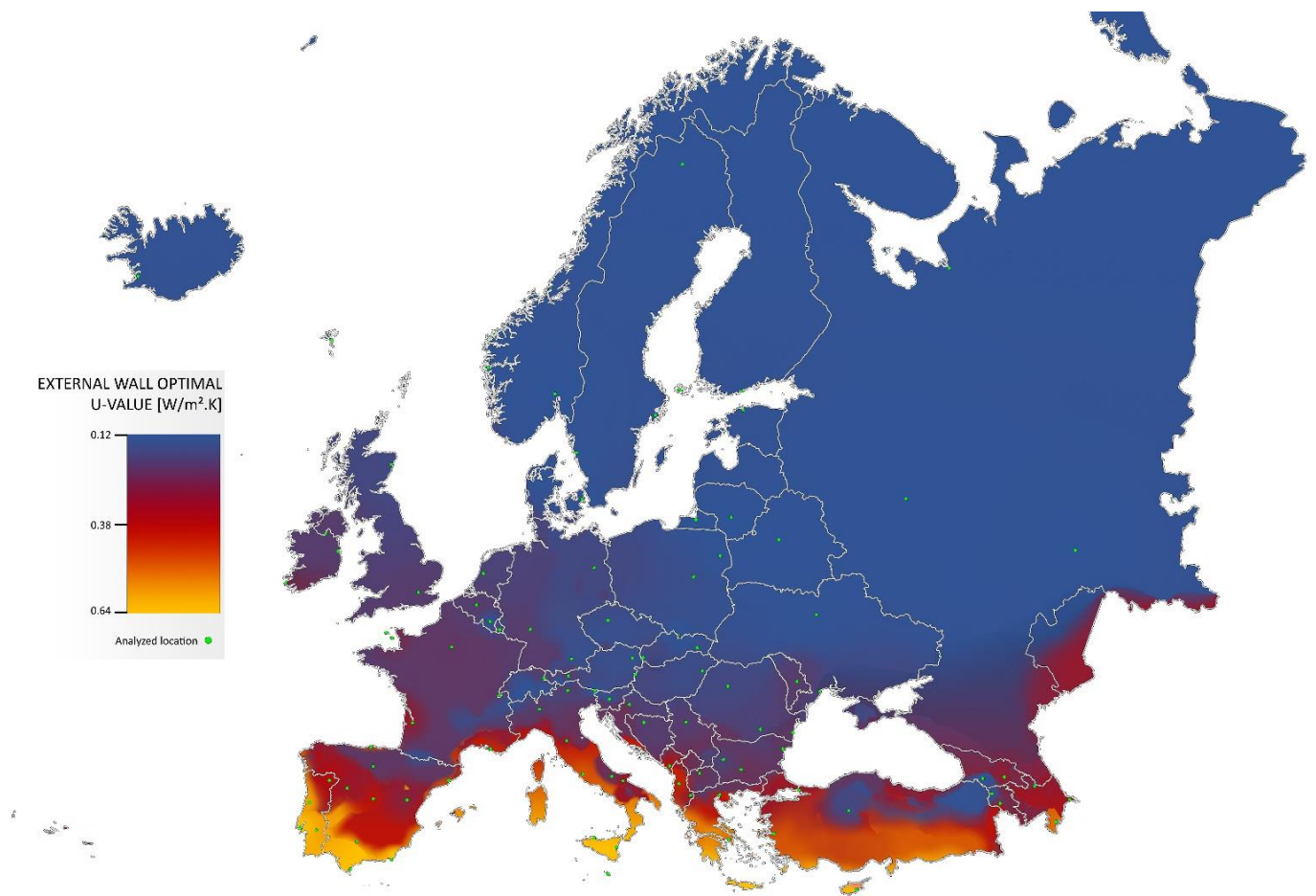


Figure 9. Optimal U-value map in Europe.

4. Conclusions

This work evaluates the influence of the exterior walls' thermal insulation on the energy consumption of residential buildings and defines the best U-value considering the overall primary energy consumption, taking into account both the embodied energy and operational energy in a life cycle of 30 years. Detailed results were obtained first for four reference climatic contexts, with the aim to also assess the impact of thermal mass, and subsequently for 100 locations representative of the entire European framework.

The research results show that, compared to a lightweight option, a wall with medium–high mass is the most suitable solution for all European climatic contexts, and low U-values on such wall always determine positive effects in terms of heating consumption. However, a downside effect is witnessed on the cooling energy consumption, as it may increase due to the overheating effect during the hot season. Thus, the optimal solution must be carefully identified for each location, accounting for both operational and embodied energy.

In detail, for the cold Continental climate of Oslo characterized by warm summers, where the requirements for cooling are limited, the lowest U-values on a high inertia wall are always suggested, and the energy-efficient solution is achieved at $0.12 \text{ W/m}^2\text{K}$ of the external wall's thermal transmittance. However, for moderate climates with less heating and approximately equal cooling requirements, as in the case of the oceanic temperate climate in Bordeaux, the optimal value is obtained on less extensive insulation levels (a U-value of $0.26 \text{ W/m}^2\text{K}$). For hot climates, the thermal inertia's effect on cooling becomes more relevant, and increasing the wall's insulation beyond a defined threshold will negatively impact the energy balance. In such terms, as shown in the results for Rome, characterized by a hot-summer Mediterranean climate, a good balance with heating reduction from

insulation is achieved at a thermal transmittance level of $0.42 \text{ W/m}^2\text{K}$. Nevertheless, for the case of hot regions characterized by semi-arid climates such as the representative example of Almeria, a massive wall with little to no insulation is preferable, for an optimal solution of $0.64 \text{ W/m}^2\text{K}$. Moreover, it should be noted that these values may fluctuate based also on the latitude that affects the amount of solar radiation and if the location is presented within an intermediate zone in proximity to two adjacent climates.

The positive effect of thermal capacity appears to be relevant for moderate climates (e.g., southern Europe and the Mediterranean area) and intermediate seasons, where it can work as a stabilizing factor of the thermal dynamics of the whole building system.

Additionally, it should be noted that the impact of the embodied energy on the overall energy consumption is climate dependent: in heating-dominated regions, the embodied energy represents a smaller percentage in the life-cycle energy use, while in temperate climates, the impact due to the material is pivotal in order to define the best optimal solution.

It is always worth noting that the embodied energy, building size, thermal performance and external-wall configuration affect the definition of the optimal U-value. It is therefore necessary to address further considerations for these elements in the specialistic energy design of the buildings. Therefore, the following limitation of the present study should be underlined:

- the building is a prototype adopted to represent mid-rise multifamily residential buildings along Europe. Its model is isolated (there are no obstruction in respect to the sky dome or the surrounding context) with a fixed orientation and does not consider a shading system for transparent surfaces;
- one single building operation and internal gains profile was considered;
- the weather data files used for the HDD and CDD calculation and the energy simulation are based on historical data, some of which present outdated information (e.g., for Italy, IGDG weather data collection is based on a 1951–1970 period of records);
- the optimal solution was calculated based on the overall energy consumption obtained from the massive wall variant only; hence, different results can be obtained by changing the wall's stratification settings;
- the polyisocyanurate foam board was adopted as a reference insulant, and an average embodied energy across Europe was considered. Alternative insulation solutions with a different embodied impact would lead to slightly different results.

Author Contributions: Conceptualization, S.O., N.A., C.D.P. and F.L.; methodology, S.O., F.M.B., N.A., C.D.P., F.L. and R.S.A.; software, S.O. and F.L.; validation, S.O., C.D.P. and F.L.; formal analysis; S.O., C.D.P. and F.L.; investigation, S.O., C.D.P. and F.L.; resources, N.A., C.D.P. and F.L.; data curation, S.O.; writing—original draft preparation, S.O. and F.L.; writing—review and editing, S.O., N.A., C.D.P. and F.L.; visualization, S.O. and F.L.; supervision, N.A., C.D.P., R.S.A. and F.M.B. All authors have read and agreed to the published version of the manuscript.

Funding: This study and project is financially supported by EU Research and Innovation programme Horizon 2020 through number 768921—HEART. The authors would like to thank the European Commission to enable the funding of this project.

Data Availability Statement: Not applicable.

Conflicts of Interest: The authors declare no conflict of interest.

References

1. United Nations Environment Programme. 2021 Global Status Report for Buildings and Construction: Towards a Zero-Emission, Efficient and Resilient Buildings and Construction Sector. 2021. Nairobi. Available online: https://globalabc.org/sites/default/files/2021-10/GABC_Buildings-GSR-2021_BOOK.pdf (accessed on 26 April 2022).
2. European Commission. Joint Research Centre. Institute for Energy and Transport Heat and Cooling Demand and Market Perspective. LU: Publications Office. 2012. Available online: <https://data.europa.eu/doi/10.2790/56592> (accessed on 12 March 2022).
3. European Environment Agency. Climate Change, Impacts and Vulnerability in Europe 2012: An Indicator Based Report. LU: Publications Office. 2012. Available online: <https://data.europa.eu/doi/10.2800/66071> (accessed on 12 March 2022).

4. Castellari, S.; Venturini, S.; Ballarin Denti, A.; Bigano, A.; Bindi, M.; Bosello, F.; Carrera, L.; Chiriaco, M.V.; Danovaro, R.; Desiato, F.; et al. *Rapporto Sullo Stato delle Conoscenze Scientifiche su Impatti, Vulnerabilità ed Adattamento ai Cambiamenti Climatici in Italia*; Ministero dell’Ambiente e della Tutela del Territorio e del Mare: Roma, Italy, 2014; p. 878.
5. Energy Technology Perspectives 2020—Analysis. IEA. Available online: <https://www.iea.org/reports/energy-technology-perspectives-2020> (accessed on 1 April 2022).
6. European Climate Foundation. *Roadmap 2050: A Practical Guide to a Prosperous Low Carbon Europe*; European Climate Foundation: The Hague, The Netherlands, 2010.
7. Action de l’UE Pour le Climat et Pacte Vert Pour l’Europe. Available online: https://ec.europa.eu/clima/eu-action/european-green-deal_fr (accessed on 12 March 2022).
8. Economidou, M.; Atanasiu, B.; Despret, C.; Maio, J.; Nolte, I.; Rapf, O.; Laustsen, J.; Ruysssevelt, P.; Staniaszek, D.; Strong, D.; et al. *Europe’s Buildings under the Microscope. A Country-by-Country Review of the Energy Performance of Buildings*; Buildings Performance Institute Europe BPIE: Brussels, Belgium, 2011.
9. Silvestre, J.D.; Castelo, A.M.P.; Silva, J.J.B.C.; de Brito, J.M.C.L.; Pinheiro, M.D. Retrofitting a Building’s Envelope: Sustainability Performance of ETICS with ICB or EPS. *Appl. Sci.* **2019**, *9*, 1285. [\[CrossRef\]](#)
10. Rivoire, M.; Casasso, A.; Piga, B.; Sethi, R. Assessment of Energetic, Economic and Environmental Performance of Ground-Coupled Heat Pumps. *Energies* **2018**, *11*, 1941. [\[CrossRef\]](#)
11. D’Agostino, D.; Rossi, F.D.; Marigliano, M.; Marino, C.; Minichiello, F. Evaluation of the optimal thermal insulation thickness for an office building in different climates by means of the basic and modified ‘cost-optimal’ methodology. *J. Build. Eng.* **2019**, *24*, 100743. [\[CrossRef\]](#)
12. Aste, N.; Leonforte, F.; Manfren, M.; Mazzon, M. Thermal inertia and energy efficiency—Parametric simulation assessment on a calibrated case study. *Appl. Energy* **2015**, *145*, 111–123. [\[CrossRef\]](#)
13. Ingraio, C.; Messineo, A.; Beltramo, R.; Yigitcanlar, T.; Ioppolo, G. How can life cycle thinking support sustainability of buildings? Investigating life cycle assessment applications for energy efficiency and environmental performance. *J. Clean. Prod.* **2018**, *201*, 556–569. [\[CrossRef\]](#)
14. Sartori, I.; Hestnes, A.G. Energy use in the life cycle of conventional and low-energy buildings: A review article. *Energy Build.* **2007**, *39*, 249–257. [\[CrossRef\]](#)
15. Kumar, D.; Alam, M.; Zou, P.X.W.; Sanjayan, J.G.; Memon, R.A. Comparative analysis of building insulation material properties and performance. *Renew. Sustain. Energy Rev.* **2020**, *131*, 110038. [\[CrossRef\]](#)
16. Tukhtamisheva, A.; Adilova, D.; Banionis, K.; Levinskytė, A.; Bliudzius, R. Optimization of the Thermal Insulation Level of Residential Buildings in the Almaty Region of Kazakhstan. *Energies* **2020**, *13*, 4692. [\[CrossRef\]](#)
17. *Guidelines Accompanying Commission Delegated Regulation (EU) No 244/2012 of 16 January 2012 Supplementing Directive 2010/31/EU of the European Parliament and of the Council on the Energy Performance of Buildings by Establishing a Comparative Methodology Framework for Calculating Cost-Optimal Levels of Minimum Energy Performance Requirements for Buildings and Building Elements*; European Commission: Brussels, Belgium, 2012; p. 28.
18. Moradiboustouni, M.; Vale, B.; Isaacs, N. A life cycle study of insulation in a case study building with a focus on the effect of the national energy profile. *J. Build. Eng.* **2021**, *43*, 103178. [\[CrossRef\]](#)
19. Chen, Z.; Hammad, A.W.A.; Kamardeen, I.; Akbarnezhad, A. Optimising Embodied Energy and Thermal Performance of Thermal Insulation in Building Envelopes via an Automated Building Information Modelling (BIM) Tool. *Buildings* **2020**, *10*, 218. [\[CrossRef\]](#)
20. Raouf, A.M.; Al-Ghamdi, S.G. Effect of R-values changes in the baseline codes: Embodied energy and environmental life cycle impacts of building envelopes. *Energy Rep.* **2020**, *6*, 554–560. [\[CrossRef\]](#)
21. Cusenza, M.A.; Gulotta, T.M.; Mistretta, M.; Cellura, M. Life Cycle Energy and Environmental Assessment of the Thermal Insulation Improvement in Residential Buildings. *Energies* **2021**, *14*, 3452. [\[CrossRef\]](#)
22. Sierra-Pérez, J.; Rodríguez-Soria, B.; Boschmonart-Rives, J.; Gabarrell, X. Integrated life cycle assessment and thermodynamic simulation of a public building’s envelope renovation: Conventional vs. Passivhaus proposal. *Appl. Energy* **2018**, *212*, 1510–1521. [\[CrossRef\]](#)
23. Bojić, M.; Miletić, M.; Bojić, L. Optimization of thermal insulation to achieve energy savings in low energy house (refurbishment). *Energy Convers. Manag.* **2014**, *84*, 681–690. [\[CrossRef\]](#)
24. Ramesh, T.; Prakash, R.; Shukla, K.K. Life cycle energy analysis of a residential building with different envelopes and climates in Indian context. *Appl. Energy* **2012**, *89*, 193–202. [\[CrossRef\]](#)
25. Shadram, F.; Bhattacharjee, S.; Lidelöv, S.; Mukkavaara, J.; Olofsson, T. Exploring the trade-off in life cycle energy of building retrofit through optimization. *Appl. Energy* **2020**, *269*, 115083. [\[CrossRef\]](#)
26. Roudsari, M.S.; Pak, M. Ladybug: A parametric environmental plugin for grasshopper to help designers create an environmentally-conscious design. In Proceedings of the 13th International IBPSA Conference, Lyon, France, 26–28 August 2013; pp. 3128–3135.
27. Sousa, J. *Energy Simulation Software for Buildings: Review and Comparison*; Faculdade de Engenharia da Universidade do Porto: Porto, Portugal, 2012.
28. Landolfo, R.; Formisano, A.; di Lorenzo, G.; di Filippo, A. Classification of european building stock in technological and typological classes. *J. Build. Eng.* **2022**, *45*, 103482. [\[CrossRef\]](#)

29. A Forward Looking Primary Energy Factor for a Greener European Future. Available online: https://www.eurelectric.org/media/2382/2018_industry_association_position_on_pef_revision-2018-030-0114-01-e-h-216CBE01.pdf (accessed on 1 April 2022).
30. EnergyPlus. Available online: <https://energyplus.net/weather> (accessed on 1 April 2022).
31. *Meteonorm Software*; Meteotest SA: Berne, Switzerland, 2020.
32. Peel, M.C.; Finlayson, B.L.; McMahon, T.A. Updated world map of the Köppen-Geiger climate classification. *Hydrol. Earth Syst. Sci.* **2007**, *11*, 1633–1644. [[CrossRef](#)]
33. Loga, T.; Diefenbach, N. *Use of Building Typologies for Energy Performance Assessment of National Building Stocks. Existent Experiences in European Countries and Common Approach*; Institut Wohnen und Umwelt: Darmstadt, Germany, 2010.
34. Zangheri, P.; Armani, R.; Pietrobon, M.; Pagliano, L.; Boneta, M.F.; Müller, A. *Heating and Cooling Energy Demand and Loads for Building Types in Different Countries of the EU*; Intelligent Energy Europe Programme of the European Union: Brussels, Belgium, 2014.
35. Smolinski, F. Renovating the Existing Building Stock across Europe—BSRIA Webinar and Building Stock Analysis. iNSPiRe. Available online: <https://inspire-fp7.eu/renovating-the-existing-building-stock-across-europe-bsria-webinar-and-building-stock-analysis/> (accessed on 12 March 2022).
36. Manfren, M.; Aste, N.; Leonforte, F.; Del Pero, C.; Buzzetti, M.; Adhikari, R.S.; Zhixing, L. Parametric energy performance analysis and monitoring of buildings—HEART project platform case study. *Sustain. Cities Soc.* **2020**, *61*, 102296. [[CrossRef](#)]
37. Pohoryles, D.A.; Maduta, C.; Bournas, D.A.; Kouris, L.A. Energy performance of existing residential buildings in Europe: A novel approach combining energy with seismic retrofitting. *Energy Build.* **2020**, *223*, 110024. [[CrossRef](#)]
38. *SIA Merkblatt 2024, Raumnutzungsbedingungen für die Energie- und Gebäudetechnik*; Schweizerischer Ingenieur- und Architektenverein: Zürich, Switzerland, 2015.
39. Nazaroff, W. Residential air-change rates: A critical review. *Indoor Air* **2021**, *31*, 282–313. [[CrossRef](#)] [[PubMed](#)]
40. EN 15251:2007—Indoor Environmental Input Parameters for Design and Assessment of Energy Performance of Buildings Addressing Indoor Air Quality, Thermal Environment, Lighting and Acoustics. iTeh Standards Store. Available online: <https://standards.itih.ai/catalog/standards/cen/92485123-bf64-40e3-9387-9724a642eae8/en-15251-2007> (accessed on 1 April 2022).
41. European Commission. Joint Research Centre. Competitive Landscape of the EU’s Insulation Materials Industry for Energy-Efficient Buildings: Revised Edition. LU: Publications Office. 2018. Available online: <https://data.europa.eu/doi/10.2760/750646> (accessed on 12 March 2022).